The Region Preceding the C-Terminal NWETF Pentapeptide Modulates Baseline Activity and Aspartate Inhibition of *Escherichia coli* Tar[†]

Run-Zhi Lai, Arjan F. Bormans, Roger R. Draheim, Gus A. Wright, and Michael D. Manson*

Department of Biology, 3258 TAMU, Texas A&M University, College Station, Texas 77843

Received July 15, 2008; Revised Manuscript Received October 20, 2008

ABSTRACT: The Tar chemoreceptor−CheA−CheW ternary complex of *Escherichia coli* is a transmembrane allosteric enzyme in which binding of ligands to the periplasmic domain modulates the activity of CheA kinase. Kinase activity is also affected by reversible methylation of four glutamyl residues in the cytoplasmic domain of the receptor. *E. coli* Tar contains 553 residues. Residues 549−553 comprise the NWETF pentapeptide that binds the CheR methyltransferase and CheB methylesterase. The crystal structure of the similar Tsr chemoreceptor predicts that residues 263−289 and 490−515 of Tar form the most membrane-proximal portion of the extended CD1−CD2 four-helix bundle of the cytoplasmic domain. The last methylation site, Glu-491, is in the C19 heptad, and the N22-19 and C22-19 heptads are present in all classes of bacterial transmembrane chemoreceptors. Residues 516−548 probably serve as a flexible tether for the NWETF pentapeptide. Here, we present a mutational analysis of residues 505−548. The more of this region that is deleted, the less sensitive Tar is to inhibition by aspartate. Tar deleted from residue 505 through the NWETF sequence stimulates CheA in vitro but is not inhibited by aspartate. Thus, interaction of the last two heptads (C21 and C22) of CD2 with the first two heptads (N22 and N21) of CD1 must be important for transmitting an inhibitory signal from the HAMP domain to the four-helix bundle. The R514A, K523A, R529A, R540A, and R542A substitutions, singly or together, increase the level of activation of CheA in vitro, whereas the R505A substitution decreases the level of CheA stimulation by 40% and lowers the aspartate K_i 7-fold. The R505E substitution completely abolishes stimulation of CheA in vitro. Glu-505 may interact electrostatically with Asp-273 to destabilize the "on" signaling state by loosening the four-helix bundle.

Bacterial chemotaxis is the best-developed model system for transmembrane signal transduction. Like many other signaling systems, bacterial chemotaxis regulates a protein kinase (*1*). This regulation is carried out by a group of transmembrane chemoreceptors that transmit signals into the cytoplasm. In *Escherichia coli*, there are four membrane-spanning, homodimeric chemoreceptors: Tar, Tsr, Tap, and Trg. The intracellular level of the high-abundance receptors Tar and Tsr is ∼20-fold higher than that of the low-abundance receptors, Trg and Tap (*2*). All of these receptors contain a periplasmic domain, a transmembrane region, and a large cytoplasmic domain (Figure 1A).

The majority of the cytoplasmic domain consists of two antiparallel α-helices (CD1[1] and CD2), which form an extended four-helix bundle hairpin within the dimer (*3*−*5*). Proceeding from the membrane into the cytoplasm, the cytoplasmic domain features the HAMP linker, the methylation subdomain, and the kinase activation subdomain (Figure 1). The HAMP linker contains two predicted amphipathic α-helices and connects the second transmembrane helix (TM2) to the cytoplasmic subdomains (*6*−*8*). The methylation subdomain contains the four glutamyl residues that serve as methylation sites in Tar.

The chemoreceptors form trimers of dimers (*3, 4*) that localize to the cell pole and form tight clusters there in the presence of CheA and CheW (*9, 10*). Trimers may contain dimers of different receptor types (*11*) and are apparently organized into large signaling lattices that obligatorily contain CheA and CheW (*12*) and also at least some of the CheR, CheB, CheY, and CheZ proteins of the cell.

The interaction of the CheA kinase with the kinase-activation domain of the receptor requires the coupling protein CheW. A ternary complex, consisting of the receptor, CheW, and CheA, is active in its apo form and is regulated by the binding of attractant (inhibitory ligand) or repellent (activating ligand) to the receptor (*1*). The receptor stimulates ATP-dependent autophosphorylation of CheA, which transfers the phosphoryl group to the response regulator CheY. Binding of phospho-CheY to the FliM protein in the C-ring of the flagellar motor increases the probability of clockwise (CW) flagellar rotation and promotes tumbling by the cell (*13*). Phosphorylation of CheY is reversed by the phosphatase CheZ (*14*). The intracellular concentration of phospho-CheY

[†] This work was supported by a grant from the National Institutes of Health (Grant GM39736 to M.D.M.) and by the Bartoszek Fund for Basic Biological Science.

* To whom correspondence should be addressed. Telephone: (979) 845-5158. Fax: (979) 845-2981. E-mail: mike@mail.bio.tamu.edu.

[1] Abbreviations: CD1, cytoplasmic domain helix 1; CD2, cytoplasmic domain helix 2; HAMP, domain for histidine kinases, adenylyl cyclases, methyl-accepting proteins, and phosphatases; TM2, transmembrane helix 2; C-ring, cytoplasmic ring; CCW, counterclockwise; CW, clockwise; IPTG, isopropyl β-D-thiogalactopyranoside; Amp, ampicillin; SDS−PAGE, sodium dodecyl sulfate−polyacrylamide gel electrophoresis.

10.1021/bi8013399 CCC: $40.75
Published on Web 11/17/2008

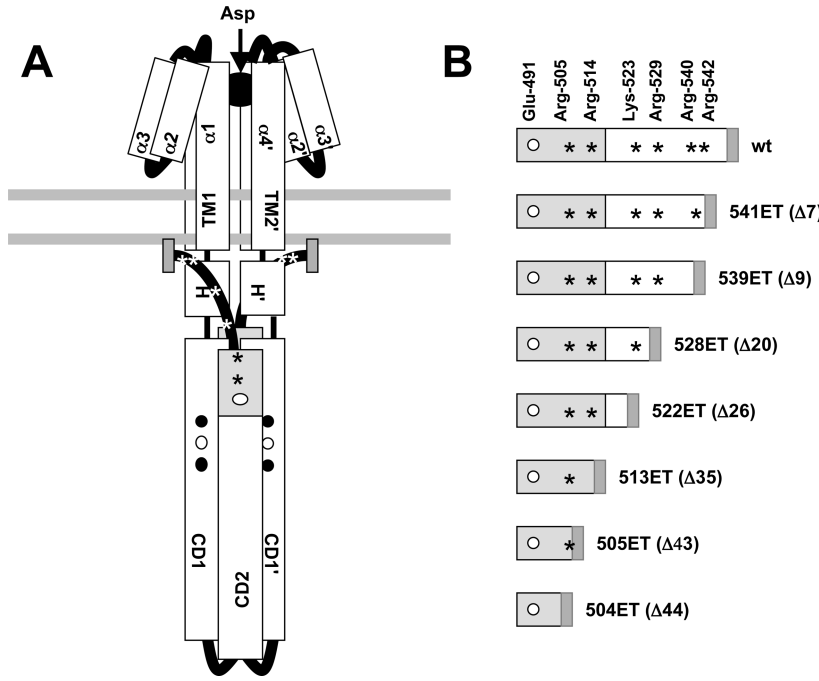

FIGURE 1: Schematic view of the Tar chemoreceptor showing engineered C-terminal truncations and residue substitutions. (A) Model of the receptor homodimer based on crystal structures of the periplasmic domain of *Salmonella* Tar (*49*) and the cytoplasmic domain of *E. coli* Tsr (*3*). Structures for the TM domain, the C-terminal flexible region, and the HAMP domain in the intact receptor are not available. Components in the subunit at the right are indicated with primes. Starting at the N-terminus, each monomer consists of transmembrane helix 1 (TM1), a periplasmic domain that is a four-helix bundle (α1−α4), transmembrane helix 2 (TM2), a HAMP linker domain (H), a helical hairpin comprising the descending CD1 helix and the ascending CD2 helix, and a disordered tail (thick black line) with the NWETF CheR-binding motif (dark gray) at its C-terminal end. Residues 490−515 are highlighted in light gray; Glu-491 (the last methylation site) is depicted as a white circle, and the approximate positions of the six basic amino acids in the last 50 residues are denoted with asterisks. (B) Last 63 residues of *E. coli* Tar. Asterisks denote the relative positions of the six basic residues indicated in panel A. The NWETF pentapeptide is depicted as a gray box, and the methylation sites are shown as circles; those translated as Gln residues are colored black, and those translated as Glu are colored white. Endotruncations (ET) extend from one of the basic residues to just before the NWETF motif. To facilitate comparison with the study of Li and Hazelbauer (*23*), the number of residues deleted for each endotruncation is given in parentheses. The corresponding complete truncations (CT) have the same N-terminal ends but are deleted through the NWETF pentapeptide.

determines the ratio of CW to counterclockwise (CCW) rotation and the run-tumble swimming behavior of the cell (*15*).

The receptor−CheW−CheA ternary complex can be viewed as an allosteric enzyme (*16*). It has been proposed that there are two states of the enzyme: "on" and "off". The equilibrium between these states is affected by several factors: ligand binding, methylation, association with CheA and CheW, and association with other receptors in a large signaling cluster (*1, 12*). Attractant binding to the receptor causes an inactivation of CheA that can be reversed by an increased level of methylation. However, the mechanisms by which ligand binding and methylation work together to regulate CheA remain unclear.

Methylation by the CheR methyltransferase and demethylation by the CheB methylesterase determine the steady-state methylation level of the receptors and allow *E. coli* to adapt to stimuli and respond over a wide range of chemoeffector concentrations (*17, 18*). Efficient adaptation requires the NWETF pentapeptide, which comprises the last five C-terminal residues of Tar and Tsr, binds CheR (*19*−*21*), and stimulates the activity of CheB (*22*).

Approximately 50 residues separate the last methylation site (Glu-491) from the NWETF pentapeptide in *E. coli* Tar. A deletion analysis of the last 40 residues of this region by Li and Hazelbauer (*23*) indicated that they act as a flexible tether. The disordered state of the last ∼30 residues in this region in the crystal structure of Tsr is consistent with this function. However, this region may also play other roles in receptor function. To address this possibility, we created a series of deletions, the longest beginning with Arg-505, that either remove or retain the NWETF motif. We also created single and combined Ala substitutions at the six basic residues in the region as well as the R505E replacement. The in vivo and in vitro properties of the mutant receptors were then examined. In addition to confirming the conclusions of Li and Hazelbauer (*23*), our analysis suggests that residues 505−515 help to determine the baseline signaling state of the receptor and control its ability to be inhibited by aspartate.

EXPERIMENTAL PROCEDURES

Strains and Plasmids. Strain RP3098 [Δ(*flhD-flhB*)4] (*24*), a derivative of *E. coli* K12 strain RP437 (*25*), was used to prepare membranes containing high levels of chemoreceptors. It was also used to express the CheA protein for purification. Another derivative of RP437, strain VB13 (*thr*+ *eda*+ Δ*tsr7201 trg*::Tn10 Δ*tar-tap5201*), was used for assays of chemotaxis (*26*). Strain BL21(λDE3) (Novagen) was used to produce CheY and CheW for purification. The λDE3 derivative of BL21 [F^- *ompT* $hsdS_B$ ($r_B^-m_B^-$) *gal dcm*] contains a prophage that encodes the T7 RNA polymerase gene under the control of the *lacUV5* promoter.

Plasmids pDM011 and pRD400 both are derivatives of pET24a(+) and contain the *cheY* and *cheW* genes, respectively, expressed from the T7 promoter. Plasmid pKJ9 carries a *cheA* gene that can be induced by isopropyl β-D-thiogalactopyranoside (IPTG). Plasmid pCJTar was constructed by cloning wild-type *E. coli tar* into pCJ30, in which it is expressed under control of a *tac* (IPTG-inducible) promoter. Plasmid pMK113 (Amp^r), a derivative of pBR322, carries *E. coli tar* under control of a modified *tar* (*meche* operon) promoter (*27*). VB13 containing pMK113 carries out good chemotaxis to aspartate and maltose. Mutations were introduced into *tar* carried on plasmids pCJ30 and pMK113 using the site-directed mutagenesis protocol from Stratagene.

Chemotaxis Ring Formation Assay. The assay was performed as described previously (*28*), using strain VB13 containing pMK113 or one of its mutant derivatives. The diameter of chemotactic rings was measured at 30 °C at 4 h intervals from the time a ring first became visible for cells expressing wild-type Tar, and chemotaxis was scored as the rate of increase in swarm diameter in millimeters per hour. Each mutant was assayed in triplicate.

In Vivo Receptor-Methylation Assay. Receptor methylation was analyzed according to Draheim et al. (*28*), using strain VB13 containing pMK113 or one of its mutant derivatives. Tar was detected on the nitrocellulose membrane with anti-Tsr antiserum (primary) and goat anti-rabbit antibody conjugated with alkaline phosphatase (secondary) (*26*). The methylation state was determined from the position of the bands visualized on the immunoblot. The migration rate of Tar during SDS−PAGE correlates with the extent of methylation, with the more highly methylated species migrating faster. An equal mix of the EEEE, QEQE, and QQQQ forms of Tar, contained in membrane preparations made from strain RP3098 bearing the appropriate plasmid, was used as a standard.

Purification of Chemotaxis Proteins. CheA and CheY were purified as described previously (*28*). CheW purification was based on the methods of Hess et al. (*29*) and Stock et al. (*30*). Cytoplasmic membranes containing overexpressed receptors were prepared as described previously (*31*), with the following modifications. The harvested cells were treated with 100 μg/mL egg white lysozyme on ice for 30 min before being lysed in a French pressure cell operated at 10000 psi. The lysate was centrifuged at 1200*g* for 15 min to remove debris. Membranes were pelleted by centrifugation at 30000*g* for 1 h, washed, and resuspended in 2 mL of a 25% (w/v) sucrose solution. The membranes were then fractionated, dialyzed, analyzed, and stored as described previously (*31*).

In Vitro CheA-Kinase Assay. The receptor-coupled CheA assay was performed as described previously (*31*), as was ligand-dependent inhibition of CheA activity. Receptor, CheA, CheW, and CheY were present at 250 nM, 62.5 nM, 250 nM, and 6.25 mM, respectively, in a total volume of 8 μL. Activities were normalized for the ratio of receptor to total membrane protein in each sample, since activity is proportional to that ratio (*31*). The experimental data for the aspartate titration of activity were fitted with the Hill equation, using Origin, version 7.0. The apparent K_i and the Hill coefficient, n_H, were determined using the Levenberg−Marquardt method with Origin. Standard deviations from the mean for K_i and n_H (Hill coefficient) values were calculated from at least three experiments.

RESULTS

Internal Deletions at the C-Terminus of Tar. The C-terminus of *E. coli* chemoreceptors is presumed to be far from both the periplasmic ligand-binding and the CheA-activation site at the cytoplasmic tip of the receptor (Figure 1A). Much of this region is not essential for CheA stimulation, since the low-abundance chemoreceptors Trg and Tap, which have shorter C-termini and lack the NWETF pentapeptide, stimulate kinase activity as well as the high-abundance chemoreceptors when they are assayed in vitro in the amidated form in which they are originally translated (*32*; R.-Z. Lai, unpublished observations). The extreme C-terminal NWETF pentapeptide binds CheR and CheB, and a recent study (*23*) indicates that the 30 preceding residues can function as a flexible tether that allows CheR and CheB to reach the methylation sites.

E. coli Tar contains six basic amino acids in its 50 C-terminal residues: Arg-505, Arg-514, Lys-23, Arg-529, Arg-540, and Arg-542. The first two lie within the C21 and C22 heptad repeats in the region following the last methylation site (Glu-491) and are conserved in the sequences of NWETF-containing receptors from the enteric bacteria (*23*). The four remaining basic residues are not highly conserved, although all of the NWETF-containing receptors contain three or four basic residues in the flexible tether. We created two sets of deletions (Figure 1B) that remove successively larger numbers of positively charged residues. In one set, the NWETF pentapeptide at the extreme C-terminus was retained (endotruncations, designated ET), and in the other, it was removed (complete truncations, designated CT). We also constructed ET and CT deletions that begin right after Arg-505. Deletions are denoted by the position of the residue immediately preceding the deletion. Thus, 504ET and 505ET are endotruncations that remove and retain Arg-505, respectively.

Chemotaxis Mediated by C-Terminally Truncated Tar. Chemotaxis ring formation in semisolid agar was used to assess the ability of a plasmid-encoded mutant Tar protein to restore chemotaxis to transducer-deleted (ΔT) strain VB13. The wild-type and mutant receptors were expressed from a modified form of the native *tar* (*meche* operon) promoter (*27*) that supports lower rates of transcription initiation. Thus, plasmid-encoded Tar was produced in amounts only several-fold higher than that from the chromosomal *meche* operon. Chemotaxis to aspartate and maltose, and aerotaxis mediated by the chromosomally encoded Aer receptor (*33, 34*), were assessed. Only the 539ET and 541ET receptors supported reasonably good chemotaxis and aerotaxis (Figure 2). Cells expressing any of the other ET receptors formed small swarms in aspartate or maltose semisoft agar, as seen by Li and Hazelbauer (*23*), or in glycerol-only plates (to assess aerotaxis). The CT receptors, which lack the NWETF pentapeptide that makes up the CheR/CheB-binding site, all failed to support chemotaxis or aerotaxis (data not shown).

Adaptive Methylation of the ET Receptors. Adaptive methylation in vivo was assessed for each of the ET mutant Tar proteins in strain VB13. In the absence of chemoeffectors, wild-type Tar was primarily in the unmethylated state, with a small amount of singly methylated receptor also present (Figure 3). Addition of a saturating level of $NiSO_4$ (10 mM) decreased the methylation level even further,

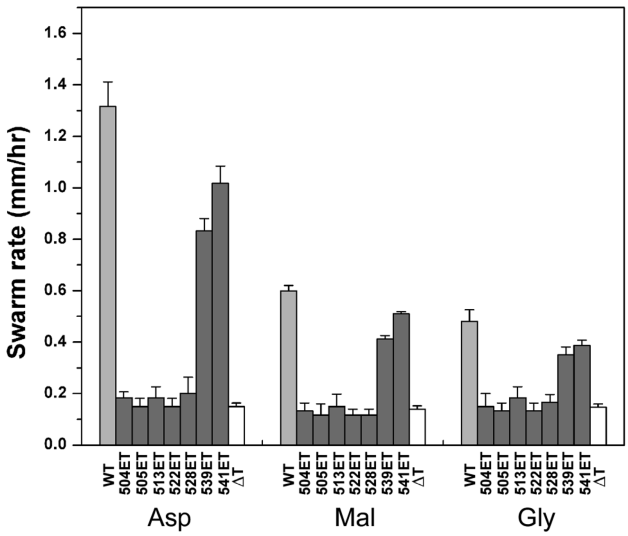

FIGURE 2: Chemotactic responses mediated by Tar receptors carrying C-terminal endotruncations (ET receptors). Rates of outward swarm-ring migration of VB13 (ΔT) cells expressing plasmid-borne wild-type or mutant *tar* genes were measured at 30 °C. Chemotaxis-ring expansion in minimal glycerol semisolid agar containing 100 μM L-aspartate, 100 μM maltose, or no additive (to assess aerotaxis) was measured in millimeters per hour. Assays were run in triplicate. Error bars represent the standard deviation of the mean.

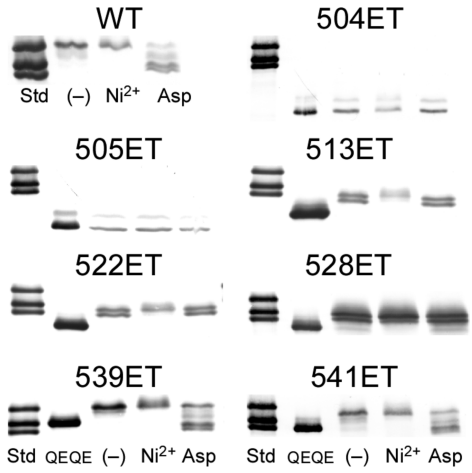

FIGURE 3: In vivo methylation of wild-type and C-terminally truncated Tar in response to chemoeffectors. Methylation of plasmid-encoded receptors was monitored in strain VB13 via immunoblotting with anti-V5 protease antibody. A sample containing equal amounts of the EEEE, QEQE, and QQQQ forms of full-length Tar and a sample containing the QEQE form of each truncated Tar are shown to the left as standards. Cells were exposed to 10 mM $NiSO_4$ (repellent), 100 mM aspartate (attractant), or buffer (−). Each lane was loaded with protein from an equal number of cells.

eliminating the faint, singly methylated band, whereas a supersaturating level of aspartate (100 mM) increased the level of methylation significantly. All the of the ET Tar proteins except the two most-truncated ones, 504ET and 505ET, were methylated to some extent in the absence of chemoeffectors, and all of these showed a decreased level of methylation after addition of 10 mM $NiSO_4$. Only the proteins with the smallest deletions, 539ET and 541ET, increased their methylation level in response to 100 mM aspartate.

Stimulation of CheA Kinase Activity by ET and CT Receptors. We next examined the behavior of the truncated Tar proteins in the in vitro receptor-coupled CheA kinase assay. In the receptor-enriched (40−60% Tar) membranes used in this assay, CheR and CheB are absent, and the receptors remain in their originally translated (QEQE) state of covalent modification at the methylation sites. In a previous study, the specific activity of receptors in stimulating CheA kinase increased linearly with the percent receptor relative to total membrane protein (*31*). Therefore, in this study, we normalized the receptor activity to the ratio of Tar to total protein for each membrane preparation.

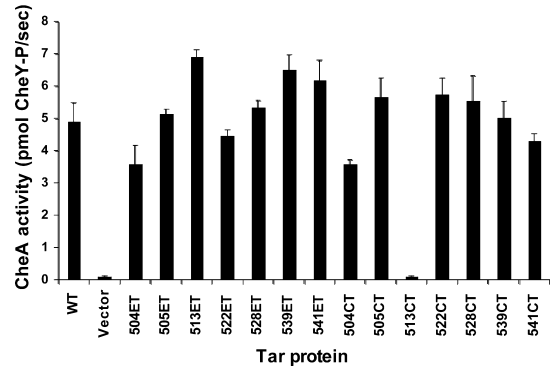

FIGURE 4: CheA stimulation by C-terminally truncated Tar receptors. CheA activity stimulated by in vitro-reconstituted receptor−CheW−CheA complexes was assayed. Activities are for 20 pmol of receptor normalized to an equal ratio of Tar to total membrane protein (see Experimental Procedures for details). Assays were run in triplicate. Error bars represent the standard deviation of the mean.

Most of the ET and CT receptors retained 80% or more of the CheA stimulating activity of wild-type Tar (Figure 4). Even the 504ET and 504CT proteins had 70% of the wild-type activity. The only exception was the 513CT protein, which was only 5% as active as the wild type. None of the truncated proteins were degraded significantly (data not shown). Since no additional mutations were found in a whole-gene sequencing, the low activity of 513CT must be due to an inherent defect in stimulating CheA, perhaps due to misfolding.

Truncated Receptors Are Less Sensitive to Inhibition by Aspartate. Aspartate titration of in vitro Tar-dependent CheA activity was used to test inhibition by attractant. Both the inhibition constant (K_i) and the cooperativity of the inhibition (n_H, the Hill coefficient) were measured. Wild-type Tar had a K_i of 7.5 ± 0.5 μM for aspartate. Both the ET and CT forms of 522, 528, 539, and 541 Tar had aspartate K_i values that were 1.2−3-fold higher (Figure 5). The 513ET and 513CT receptors exhibited a substantially higher aspartate K_i of ∼100 μM, but high concentrations of aspartate still completely inhibited their ability to stimulate CheA. Longer deletions tended to exhibit lower cooperativity. CT receptors tended to have a higher cooperativity than their ET counterparts, but this pattern was not consistent. The Hill coefficient for aspartate inhibition was between 0.9 (zero cooperativity) and 2.3, compared to the wild-type value of 2.0 (legend of Figure 5). (Recall that the baseline activity of the 513CT protein was very low to begin with.) The 504ET, 504CT, 505ET, and 505CT proteins completely lost the ability to inhibit CheA activity in the presence of aspartate.

Effect of Ala Substitutions at Basic Residues. We replaced each of the six basic residues individually with Ala. We also substituted successively greater numbers of residues per protein up through a mutant in which all six basic residues were replaced, starting with the R542A substitution and

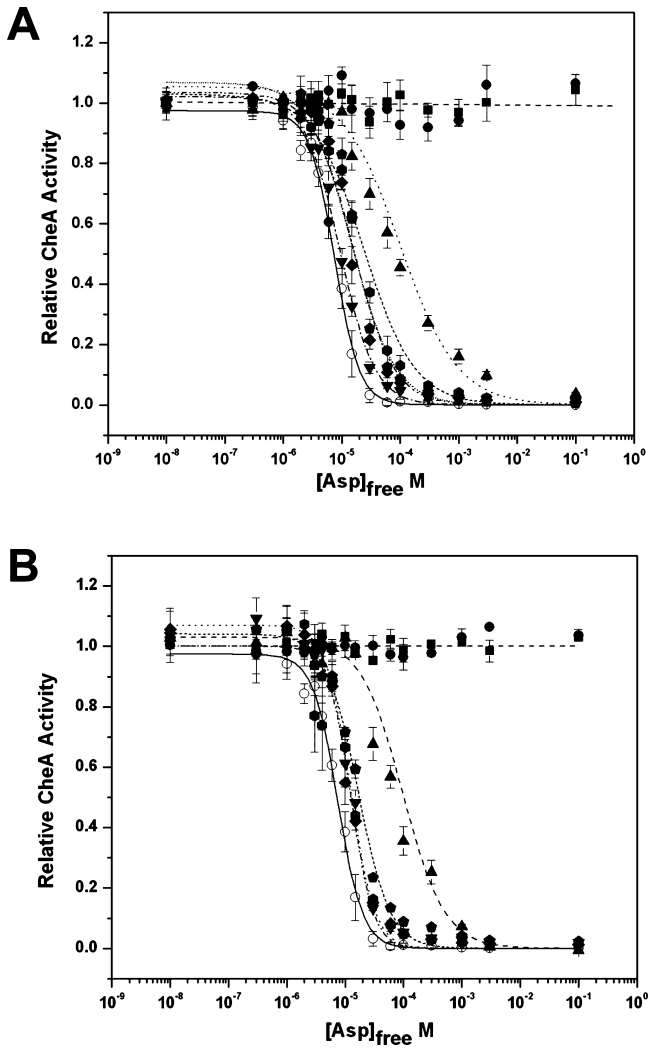

FIGURE 5: Effects of C-terminal truncations on aspartate inhibition of receptor-coupled CheA activity. The normalized CheA activities supported by (A) endotruncation (ET) or (B) complete truncation (CT) receptors were measured as a function of aspartate concentration. Best-fit inhibition curves were calculated using the Hill equation. The n_H values are given in brackets after the mutant name; no number is given when no activity could be measured: (○) wild type [2.0], (■) 504ET or CT, (●) 505ET or CT, (▲) 513ET [0.9] or CT [1.2], (▼) 522ET [1.5] or CT [2.1], (◆) 528ET [1.3] or CT [2.3], (⬣) 539ET [1.0] or CT [1.9], and (pentagons) 541ET [1.2] or CT [1.6]. Assays were run in triplicate. Error bars represent the standard deviation of the mean.

progressing stepwise in the N-terminal direction (e.g., R542A/R540A = 2A, R542A/R540A/R529A = 3A, etc.).

Chemotaxis Mediated by Ala-Substituted Tar. Plasmids expressing the Ala-substituted receptors from the modified *meche* promoter were introduced into strain VB13. All of the singly substituted receptors formed wild-type chemotactic rings in aspartate, maltose, and glycerol semisolid agar (Figure 6A). The multiply substituted proteins (Figure 6B) exhibited progressively smaller chemotactic rings on all plates, reaching a 50% decrease in the case of the 6A variant.

Adaptive Methylation of the Ala-Substituted Receptors. The in vivo methylation levels, baseline activities in the in vitro receptor-coupled CheA assay, and aspartate titration of their in vitro activity were tested for each of the Ala-substituted receptors. Most proteins had methylation patterns similar to that of wild-type Tar in the absence and presence of chemoeffectors (Figure 7). However, the R505A receptor had significantly increased levels of baseline methylation (Figure 7A), suggesting that its intrinsic signaling state may be shifted toward the off state. All of the proteins, including R505A, decreased or increased their methylation levels, respectively, upon addition of Ni^{2+} and aspartate. The multiply substituted receptors all had methylation patterns much like those of the wild type (Figure 7B), except that the multiply substituted receptors migrated somewhat more slowly in all modification states.

Stimulation of CheA Kinase Activity by Ala-Substituted Receptors. In the receptor-coupled in vitro assay, all of the singly substituted receptors (Figure 8), except R505A, had baseline activities equal to or higher than that of wild-type Tar (up to 70% higher for K523A). Tar R505A had only 60% of the activity of wild-type Tar. Similarly, the 2A−5A proteins all had higher baseline activities than wild-type Tar, with the activities being as much as 2.5-fold greater for 4A and 5A (Figure 8). However, the 6A protein had the same 60% of wild-type activity as the R505A protein.

Aspartate Inhibition of Ala-Substituted Receptors. The R505A and 6A receptors exhibited K_i values of 1.1 (Figure 9A) and 1.3 μM (Figure 9B), respectively, 7- and 6-fold lower than the K_i value of wild-type Tar of 7.5 μM (Figure 9A). In contrast, the other singly (Figure 9A) and multiply (Figure 9B) Ala-substituted receptors had aspartate K_i values somewhat higher (1.3−3-fold) than that of wild-type Tar. Thus, the higher baseline CheA stimulating activity exhibited by most of the Ala-substituted receptors correlates inversely with their ability to be inhibited by aspartate. The Hill coefficients ranged between 1.2 and 2.1, with no consistent correlation between the extent of cooperativity and the location or number of Ala substitutions.

The R505E Substitution Greatly Decreases CheA Stimulating Activity. Because of the apparent importance of the Arg-505 residue, we determined the effect of reversing the charge at this position by introducing the R505E substitution. VB13 cells expressing R505E Tar formed aspartate chemotaxis rings with only 50% of the diameter of that formed by cells expressing wild-type Tar (Figure 6A). (The swarms of VB13/R505E Tar on maltose and glycerol plates were similar to those of other strains.) Moreover, cells expressing R505E Tar had significantly sharper outer rings with aspartate. The R505E receptor in its unstimulated state was overmethylated (Figure 7A), but like R505A, it could still change its methylation state appropriately in response to addition of Ni^{2+} or aspartate.

In vitro, R505E Tar had no significant CheA-stimulating activity. Thus, the unmodified QEQE form of this receptor is strongly biased toward the off state. The ability of VB13 cells producing R505E Tar to support some level of chemotaxis in semisolid agar indicates that the increased level of adaptive methylation of the receptor seen in vivo can restore the ability of this receptor to activate CheA.

DISCUSSION

Transmembrane chemoreceptors undergo the following changes in response to binding of a chemoattractant: ligand binds; the ligand-induced conformational change is transmitted across the cell membrane; the activity of CheA associated with the kinase-activating domain is inhibited; and activity is restored by adaptive covalent methylation of the cyto-

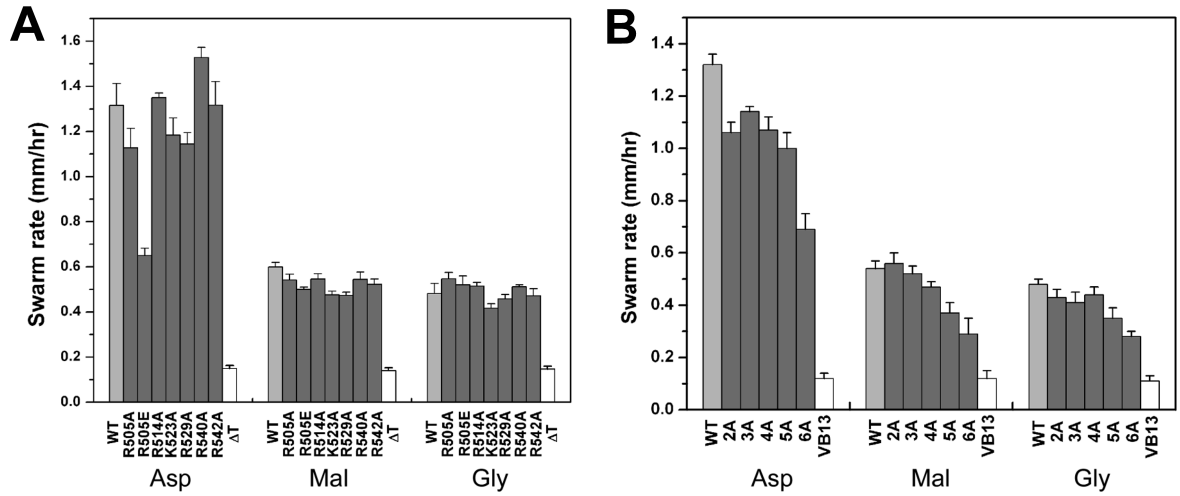

FIGURE 6: Effects on chemotactic behavior associated with substitutions at basic residues. (A) Single Ala or Glu substitutions. (B) Multiple Ala substitutions. Assays were run as described in the legend of Figure 2. Error bars represent the standard deviation of the mean.

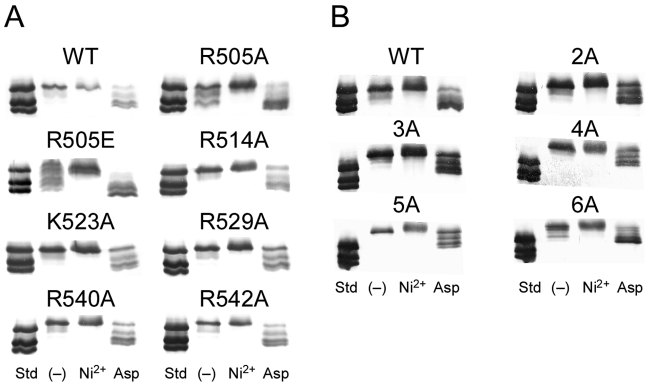

FIGURE 7: In vivo methylation of Tar receptors with residue substitutions. (A) Single-residue substitutions. (B) Multiple-residue substitutions. Assays were performed as described in the legend of Figure 3. Each lane was loaded with protein from an equal number of cells.

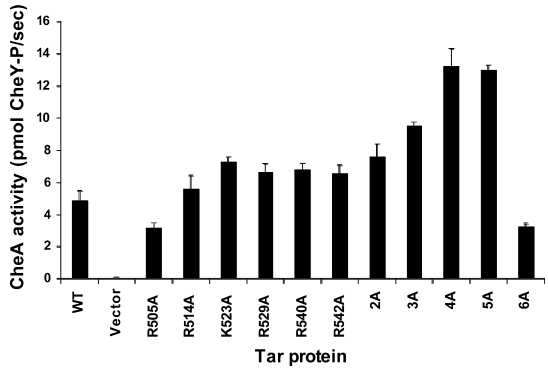

FIGURE 8: In vitro stimulation of CheA activity by Tar receptors with residue substitutions. The single-residue substitutions, shown at the left, are indicated by the actual replacements. The multiple Ala substitutions are shown at the right and are indicated by the total number of Ala replacements. Activities were normalized to an equal amount of receptor protein. Assays were run in triplicate. Error bars represent the standard deviation of the mean.

plasmic domain. Attractants interact with the periplasmic domain at specific binding sites (*1*). Small, ligand-induced, pistonlike movements of the periplasmic domain are propagated across the membrane through the second transmembrane domain of the receptor [TM2 (*35*−*38*)] and are probably amplified into larger conformational changes within the HAMP linker domain (*7, 39*). The CheA and CheW proteins interact with the membrane-distal tip of the receptor trimer of dimers (*40, 41*) in such a way that relatively subtle changes in receptor conformation increase or diminish CheA kinase activity. Methylation of Glu residues at four independent sites (*42*) leads to adaptation that cancels the ligand-induced signal by returning the receptor to its prestimulus configuration (*43*).

The most C-terminal methylation site in Tar is Glu-491 (*42*). The NWETF pentapeptide at the extreme C-terminus of Tar (residues 549−553) serves as the interaction site for the enzymes that carry out adaptive methylation and demethylation: the CheR methyltransferase (*19*−*21*) and the CheB methylesterase (*22*). The function of residues 492−548, which link the methylation subdomain and the NWETF motif (see Figure 1), is less well known. Residues beyond position 516 were not resolved in the crystal structure of the cytoplasmic domain of the closely related Tsr chemoreceptor (*3*).

In a recently published study, Li and Hazelbauer (*23*) reported the effects of internal truncations of the C-terminal region of Tar on in vitro methylation, demethylation, and deamidation. The work described here focused on the role of the C-terminal region in maintaining baseline CheA stimulation by Tar and inhibition of that activity by aspartate. Three major conclusions about the role of the receptor C-terminus can be drawn from our results.

The Last Two Heptad Repeats of CD2 Are Required for Aspartate Inhibition. The C21-22 heptads (residues 502−515), the most C-terminal in the CD2 helix, are required for aspartate sensitivity of Tar (Figure 5). Deletions extending through Arg-514 increase the aspartate K_i ~10-fold, and deletions extending to, or through, Arg-505 render the receptor blind to aspartate (Figure 5). All but the 513CT receptor retain the ability to stimulate CheA (Figure 4). We do not know their aspartate-binding affinity; however, the mutant receptors are stable, and deleted receptors that retain normal CheA-stimulating activity seem unlikely to be unable to bind aspartate. The loss of the pairing partners for the N22-21 heptads (Figure 10A), which directly follow the HAMP domain, may uncouple the four-helix bundle from conformational changes in HAMP.

We have no explanation for the very low activity of the 513CT receptor. The entire gene was sequenced, and no other mutations were found. However, the residual activity of the

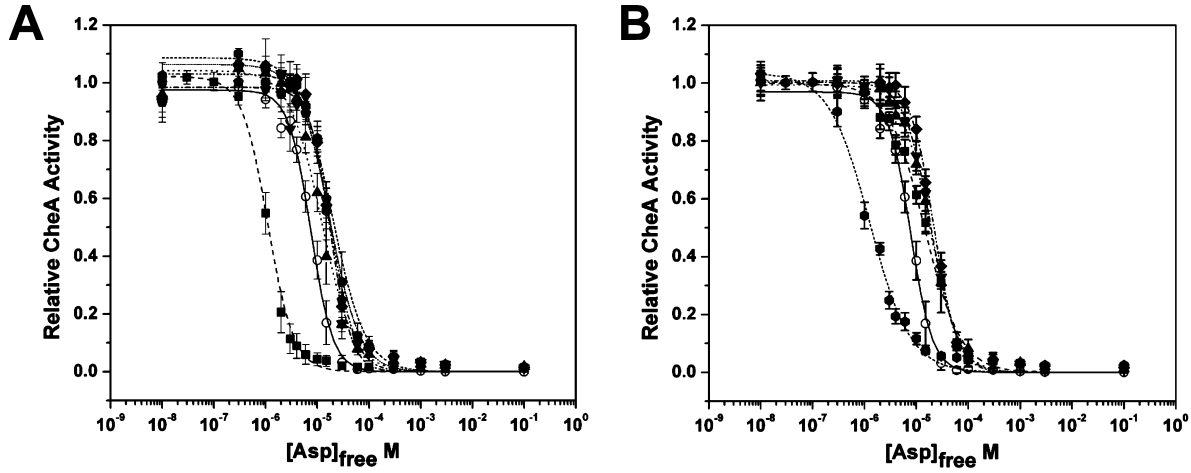

FIGURE 9: Effects of residue substitutions on aspartate inhibition of receptor-coupled CheA activity. The aspartate inhibition assay was performed as in Figure 5. (A) Single Ala substitutions. A best-fit inhibition curve was calculated using the Hill equation. The n_H values are given in brackets following the mutant designation. Symbols are: (○) wild type [2.0], (■) R505A [1.7], (▲) R514A [1.4], (▼) K523A [2.1], (◆) R529A [1.8], (●) R540A [1.4], and (pentagons) R542A [1.5]. (B) Multiple Ala substitutions: (○) wild type [2.0], (■) 2A [1.2], (▲) 3A [1.6], (▼) 4A [1.7], (◆) 5A [2.0], and (●) 6A [1.2]. Assays were run in triplicate. Error bars represent the standard deviation of the mean.

513CT protein was inhibited by aspartate in the same way as that of the fully active 513ET receptor.

Wild-type Tar in our hands has a Hill coefficient of ~2.0 for aspartate in the in vitro assay. Some of the truncated mutants, although fully active and able to be completely inhibited by high concentrations of aspartate, exhibited decreased n_H values (0.9 for the 513ET protein). The most parsimonious interpretation is that the N22−C22 interaction contributes to communication among the helices of the four-helix bundle or to interaction between dimers within the receptor trimer.

Basic Residues in the Flexible NWETF Linker Modulate CheA-Stimulating Activity. Conversion of all four basic residues in the linker (Lys-523, Arg-528, Arg-540, and Arg-542) to Ala enhances CheA-stimulating activity in vitro 250% (Figure 8). Many of the Ala-substituted receptors had decreased n_H values, but no consistent pattern was evident. The Ala replacements could either stabilize the on state of the receptor or destabilize the off state. Possible interaction targets for these residues could be the negatively charged polar headgroups of phospholipids on the cytoplasmic face of the cell membrane or charged residues elsewhere within the receptor, perhaps in the HAMP domain or the adaptation region (Figure 1). There are several charged residues on the surface of the HAMP four-helix bundle, and the N22−N19 and C19−C22 helices contain many negatively charged residues on their exposed faces (*44*).

Substitutions at Arg-505 Disrupt Kinase Stimulation. The R505A substitution decreases CheA stimulating activity by 40% and increases the sensitivity to inhibition by aspartate 7-fold. A very similar effect is seen with the 6A receptor (Figures 8 and 9). The n_H value is decreased modestly for R505A (1.7-fold) and more for the 6A receptor (1.2-fold). The R505E substitution completely eliminates the CheA-stimulating ability of the QEQE form of the receptor in vitro. Thus, neutralization of Arg-505 biases Tar toward the off state, and reversal of the positive charge to negative causes a much greater bias toward the off state. However, in vivo methylation can compensate, at least partially, for these biases (Figure 6).

Residues 263−289 of CD1 (heptads N22-19) pack in antiparallel fashion against residues 515−490 of CD2 (heptads C22-19) (*6*; J. S. Parkinson, personal communication). The residue alignments in this region of the four-helix bundle are shown in Figure 10A. The R505E substitution of Arg-505 is exactly two heptad repeats from the Glu-491 methylation site (Figure 10A) and directly opposite, and in register with, Asp-273. It has been proposed that neutralization of electrostatic repulsion can explain the mechanism of adaptive methylation (*44*); for example, methylation of Glu-491 eliminates mutual repulsion with Asp-289 (Figure 10A). Mutational neutralization of other negatively charged residues at the CD1−CD2′ interface of Tar in the adaptation domain increases the level of kinase stimulation (*44*). Apparently, a tighter bundle favors kinase activation, and a looser, more-dynamic bundle favors kinase inhibition. Thus, Glu-505 could contribute additional electrostatic repulsion that cannot be completely compensated by methylation. It will be interesting to see whether the D273R substitution, which by itself leads to a partial lock-on phenotype (*44*), reverses the effects of the R505E replacement.

HAMP and the CD1−CD2 Bundle May Communicate via Rotation. Hulko et al. (*39*) suggest, on the basis of their NMR structure of the Af1503 HAMP domain, that HAMP modulates the signaling state of receptors by a rotation of the AS1 and AS2 helices relative to one another. We propose that such a rotation may be communicated directly to CD1 and that interactions between the N-terminus of CD1 and the C-terminus of CD2′, and CD1′ and CD2, are necessary for transmission of this signal. The signaling properties of receptors lacking the C22 and C21 heptads are like those seen when the signaling and adaptation domains of Tsr are expressed by themselves (*45*). Conversely, weakening the interaction of the N22-21 and C22-21 heptads through substitutions at Arg-505 may allow HAMP to inhibit the on signaling state even in the absence of an attractant ligand, probably by loosening the CD1−CD2 four-helix bundle. This result is consistent with the conclusion, based on an extensive cysteine and disulfide-scanning analysis of residues 250−309 of the *Salmonella enterica* var. *typhimurium* Tar receptor

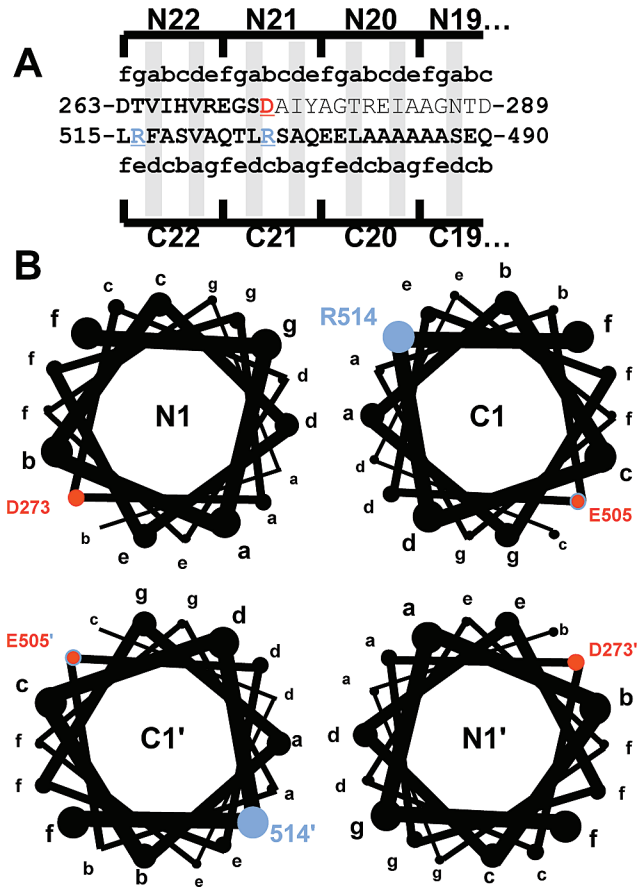

FIGURE 10: Proposed interaction of CD1 and CD2 over the N22-19 and C22-19 heptad repeats of *E. coli* Tar. (A) An alignment of N22-19 and C22-19 is shown in an antiparallel orientation, assuming a-d packing between the helices. The heptad repeat patterns (a-g and g-a) are shown above and below the amino acid sequences, which are given in single-letter code. Arg-505 and Arg-514 are colored blue and underlined. Residue Asp-273, which is in register with Arg-505, is colored red and underlined. The boundaries of the heptad repeats are shown above (for N22-19) and below (for C22-19). (B) Modeled four-helix bundle in the region of heptad repeats N22-20 (residues 263−281) and C22-20 (residues 498−515). Heptads N20 and C20 are not shown in their entirety. The model is arranged with a-d packing using the 3.6 residues/360° geometry of a free α-helix rather than the 3.5 residues/360° of a helical coiled coil; thus, the a-g positions advance ~10° for each helical turn rather than aligning along one face of the helical axis. The alignment was chosen to emphasize the possibility that the negatively charged side chains of Asp-273 and the mutationally introduced Glu-505 residue may exert electrostatic repulsion between CD1/CD2′ and CD2/CD1′ that could loosen the four-helix bundle.

(*46*), that this region of the protein is critical for control of the signaling state of the receptor.

We note that rotation of the membrane-proximal portions of the CD1−CD2 bundle can be reconciled with either the "AS1 membrane-association model" or the "gear-box rotation" model for HAMP function (*47*). It is also consistent with the recently proposed piston-triggered rotation model (*48*). Further genetic and biochemical analyses of the HAMP domain and the membrane-proximal portion of the CD1−CD2 four-helix bundle will be required to provide more information about how HAMP interfaces with the membrane-proximal portion of the cytoplasmic domain.

ACKNOWLEDGMENT

We thank John S. (Sandy) Parkinson for the generous gift of our first batches of CheA, CheW, and CheY proteins and for extremely useful conversations. Many of the ideas about CD1−CD2 interactions had their genesis in the 2008 Intermountain ReceptorFest that Sandy hosted at the University of Utah (Salt Lake City, UT). The reviewers of earlier submissions of the manuscript pointed out inconsistencies between our interpretation of our data and the published literature that have been corrected in the final version. We are grateful to all of the members in the Manson laboratory for informative discussions and inspiration. Lilia Z. K. Bartoszek proofread several versions of the manuscript and caught a number of mistakes.

REFERENCES

1. Falke, J. J., and Hazelbauer, G. L. (2001) Transmembrane signaling in bacterial chemoreceptors. *Trends Biochem. Sci. 26*, 257–265.
2. Li, M., and Hazelbauer, G. B. (2004) Cellular stoichiometry of the components of the chemotaxis signaling complex. *J. Bacteriol. 186*, 3687–3694.
3. Kim, K. K., Yokota, H., and Kim, S. H. (1999) Four-helical-bundle structure of the cytoplasmic domain of a serine chemotaxis receptor. *Nature 400*, 787–792.
4. Falke, J. J., and Kim, S. H. (2000) Structure of a conserved receptor domain that regulates kinase activity: The cytoplasmic domain of bacterial taxis receptors. *Curr. Opin. Struct. Biol. 10*, 462–469.
5. Alexander, R. P., and Zhulin, I. B. (2007) Evolutionary genomics reveals conserved structural determinants of signaling and adaptation in microbial chemoreceptors. *Proc. Natl. Acad. Aci. U.S.A. 104*, 2885–2890.
6. Butler, S. L., and Falke, J. J. (1998) Cysteine and disulfide scanning reveals two amphiphilic helices in the linker region of the aspartate chemoreceptor. *Biochemistry 37*, 10746–10756.
7. Williams, S. B., and Stewart, V. (1999) Functional similarities among two-component sensors and methyl-accepting chemotaxis proteins suggest a role for linker region amphipathic helices in transmembrane signal transduction. *Mol. Microbiol. 33*, 1093–1102.
8. Aravind, L., and Ponting, C. P. (1999) The cytoplasmic helical linker domain of receptor histidine kinase and methyl-accepting proteins is common to many prokaryotic signalling proteins. *FEMS Microbiol. Lett. 176*, 111–116.
9. Maddock, J. R., and Shapiro, L. (1993) Polar location of the chemoreceptor complex in the *Escherichia coli* cell. *Science 259*, 1717–1723.
10. Lybarger, S. R., and Maddock, J. R. (2000) Differences in the polar clustering of the high-and low-abundance chemoreceptors of *Escherichia coli*. *Proc. Natl. Acad. Sci. U.S.A. 97*, 8057–8062.
11. Studdert, C. A., and Parkinson, J. S. (2005) Insights into the organization and dynamics of bacterial chemoreceptor clusters through *in vivo* crosslinking studies. *Proc. Natl. Acad. Sci. U.S.A. 102*, 15623–15628.
12. Hazelbauer, G. L., Falke, J. J., and Parkinson, J. S. (2008) Bacterial chemoreceptors: High-performance signaling in networked arrays. *Trends Biochem. Sci. 33*, 9–19.
13. Welch, M., Oosawa, K., Aizawa, S., and Eisenbach, M. (1993) Phosphorylation-dependent binding of a signal molecule to the flagellar switch of bacteria. *Proc. Natl. Acad. Sci. U.S.A. 90*, 8787–8791.
14. Hess, J. F., Oosawa, K., Kaplan, N., and Simon, M. I. (1988) Phosphorylation of three proteins in the signaling pathway of bacterial chemotaxis. *Cell 53*, 79–87.
15. Cluzel, P., Surette, M., and Leibler, S. (2000) An ultrasensitive bacterial motor revealed by monitoring signaling proteins in single cells. *Science 287*, 1652–1655.
16. Sourjik, V. (2004) Receptor clustering and signal processing in *E. coli* chemotaxis. *Trends Microbiol. 12*, 569–576.
17. Goy, M. F., Springer, M. S., and Adler, J. (1977) Sensory transduction in *Escherichia coli*: Role of a protein methylation reaction in sensory adaptation. *Proc. Natl. Acad. Sci. U.S.A. 74*, 4964–4968.

18. Stock, J. B., and Koshland, D. E., Jr. (1978) A protein methylesterase involved in bacterial sensing. *Proc. Natl. Acad. Sci. U.S.A. 75*, 3659–3663.
19. Okumura, H., Nishiyama, S., Sasaki, A., Homma, M., and Kawagishi, I. (1998) Chemotactic adaptation is altered by changes in the carboxy-terminal sequence conserved among the major methyl-accepting chemoreceptors. *J. Bacteriol. 180*, 1862–1868.
20. Wu, J., Li, J., Li, G., Long, D. G., and Weis, R. M. (1996) The receptor binding site for the methyltransferase of bacterial chemotaxis is distinct from the sites of methylation. *Biochemistry 35*, 4984–4993.
21. Djordjevic, S., and Stock, A. M. (1998) Chemotaxis receptor recognition by protein methyltransferase CheR. *Nat. Struct. Biol. 5*, 446–450.
22. Barnakov, A. N., Barnakova, L. A., and Hazelbauer, G. L. (1999) Efficient adaptational demethylation of chemoreceptors requires the same enzyme-docking site as efficient methylation. *Proc. Natl. Acad. Sci. U.S.A. 96*, 10667–10672.
23. Li, M., and Hazelbauer, G. L. (2006) The carboxyl-terminal linker is important for chemoreceptor function. *Mol. Microbiol. 60*, 469–479.
24. Smith, R. A., and Parkinson, J. S. (1980) Overlapping genes at the cheA locus of *Escherichia coli*. *Proc. Natl. Acad. Sci. U.S.A. 77*, 5370–5374.
25. Parkinson, J. S., and Houts, S. E. (1982) Isolation and behavior of *Escherichia coli* deletion mutants lacking chemotaxis functions. *J. Bacteriol. 151*, 106–113.
26. Weerasuriya, S., Schneider, B. M., and Manson, M. D. (1998) Chimeric chemoreceptors in *Escherichia coli*: Signaling properties of Tar-Tap and Tap-Tar hybrids. *J. Bacteriol. 180*, 914–920.
27. Gardina, P., Conway, C., Kossman, M., and Manson, M. (1992) Aspartate and maltose-binding protein interact with adjacent sites in the Tar chemotactic signal transducer of *Escherichia coli*. *J. Bacteriol. 174*, 1528–1536.
28. Draheim, R. R., Bormans, A. F., Lai, R.-Z., and Manson, M. D. (2005) Tryptophan residues flanking the second transmembrane helix (TM2) set the signaling state of the Tar chemoreceptor. *Biochemistry 44*, 1268–1277.
29. Hess, J. F., Bourret, R. B., and Simon, M. I. (1991) Phosphorylation assays for proteins of the two-component regulatory system controlling chemotaxis in *Escherichia coli*. *Methods Enzymol. 200*, 188–204.
30. Stock, A., Mottonen, J., Chen, T., and Stock, J. (1987) Identification of a possible nucleotide binding site in CheW, a protein required for sensory transduction in bacterial chemotaxis. *J. Biol. Chem. 262*, 535–537.
31. Lai, R.-Z., Manson, J. M., Bormans, A. F., Draheim, R. R., Nguyen, N. T., and Manson, M. D. (2005) Cooperative signaling among bacterial chemoreceptors. *Biochemistry 44*, 14298–14307.
32. Feng, X., Baumgartner, J. W., and Hazelbauer, G. L. (1997) High- and low-abundance chemoreceptors in *Escherichia coli*: Differential activities associated with closely related cytoplasmic domains. *J. Bacteriol. 179*, 6714–6720.
33. Bibikov, S. I., Biran, R., Rudd, K. E., and Parkinson, J. S. (1997) A signal transducer for aerotaxis in *Escherichia coli*. *J. Bacteriol. 179*, 4075–4079.
34. Rebbapragada, A., Johnson, M. S., Harding, G. P., Zuccarelli, A. J., Fletcher, H. M., Zhulin, I. B., and Taylor, B. L. (1997) The Aer protein and the serine chemoreceptor Tsr independently sense intracellular energy levels and transduce oxygen, redox, and energy signals for *Escherichia coli* behavior. *Proc. Natl. Acad. Sci. U.S.A. 94*, 10541–10546.
35. Chervitz, S. A., and Falke, J. J. (1995) Lock on/off disulfides identify the transmembrane signaling helix of the aspartate receptor. *J. Biol. Chem. 270*, 24043–24053.
36. Hughson, A. G., and Hazelbauer, G. L. (1996) Detecting the conformational change of transmembrane signaling in a bacterial chemoreceptor by measuring effects on disulfide cross-linking *in vivo*. *Proc. Natl. Acad. Sci. U.S.A. 93*, 11546–11551.
37. Ottemann, K. M., Xiao, W., Shin, Y. K., and Koshland, D. E., Jr. (1999) A piston model for transmembrane signaling of the aspartate receptor. *Science 285*, 1751–1754.
38. Draheim, R. R., Bormans, A. F., Lai, R.-Z., and Manson, M. D. (2006) Tuning a bacterial chemoreceptor with protein-membrane interactions. *Biochemistry 45*, 14655–14664.
39. Hulko, M., Berndt, F., Gruber, M., Linder, J. U., Truffault, V., Schultz, A., Martin, J., Schultz, J. E., Lupas, A. N., and Coles, M. (2006) The HAMP domain structure implies helix rotation in transmembrane signaling. *Cell 126*, 929–940.
40. Liu, J. D., and Parkinson, J. S. (1991) Genetic evidence for interaction between the CheW and Tsr proteins during chemoreceptor signaling by *Escherichia coli*. *J. Bacteriol. 173*, 4941–4951.
41. Levit, M. N., Grebe, T. W., and Stock, J. B. (2002) Organization of the receptor-kinase signaling array that regulates *Escherichia coli* chemotaxis. *J. Biol. Chem. 277*, 36748–36754.
42. Terwilliger, T. C., Wang, J. Y., and Koshland, D. E., Jr. (1986) Kinetics of receptor modification. The multiply methylated aspartate receptors involved in bacterial chemotaxis. *J. Biol. Chem. 261*, 10814–10820.
43. Lai, W. C., Beel, B. D., and Hazelbauer, G. L. (2006) Adaptational modification and ligand occupancy have opposite effects of positioning of the transmembrane signaling helix of a chemoreceptor. *Mol. Microbiol. 61*, 1081–1090.
44. Starrett, D. J., and Falke, J. J. (2005) Adaptation mechanism of the aspartate receptor: Electrostatics of the adaptation subdomain play a key role in modulating kinase activity. *Biochemistry 44*, 1550–1560.
45. Ames, P., and Parkinson, J. S. (1994) Constitutively signaling fragments of Tsr, the *Escherichia coli* serine chemoreceptor. *J. Bacteriol. 176*, 6340–6348.
46. Danielson, M. A., Bass, R. B., and Falke, J. J. (1997) Cysteine and disulfide scanning reveals a regulatory α helix in the cytoplasmic domain of the aspartate receptor. *J. Biol. Chem. 272*, 32878–32888.
47. Manson, M. D. (2008) The tie that binds the dynamic duo: The connector between AS1 and AS2 in the HAMP domain of the *E. coli* Tsr chemoreceptor. *J. Bacteriol. 190*, 6544–6547.
48. Swain, K. E., and Falke, J. J. (2007) Structure of the conserved HAMP domain in an intact, membrane-bound chemoreceptor: A disulfide mapping study. *Biochemistry 46*, 13684–13695.
49. Milburn, M. V., Prive, G. G., Milligan, D. L., Scott, W. G., Yeh, J., Jancarik, J., Koshland, D. E., Jr., and Kim, S. H. (1991) Three-dimensional structures of the ligand-binding domain of the bacterial aspartate receptor with and without a ligand. *Science 254*, 1342–1347.

BI8013399